

UCSF

UC San Francisco Previously Published Works

Title

Interactions of Age and Blood Immune Factors and Noninvasive Prediction of Glioma Survival

Permalink

<https://escholarship.org/uc/item/52v6v8z6>

Journal

Journal of the National Cancer Institute, 114(3)

ISSN

0027-8874

Authors

Molinaro, Annette M

Wiencke, John K

Warrier, Gayathri

et al.

Publication Date











2022-03-08

DOI

10.1093/jnci/djab195

Peer reviewed

Interactions of Age and Blood Immune Factors and Noninvasive Prediction of Glioma Survival

Annette M. Molinaro, PhD ^{1,2,*} John K. Wiencke, PhD,¹ Gayathri Warriar, MS ¹ Devin C. Koestler, PhD,³ Pranathi Chunduru, MS,¹ Ji Yoon Lee, BA,¹ Helen M. Hansen, BA,¹ Sean Lee, BS ¹ Joaquin Anguiano, BA,¹ Terri Rice, MPH,¹ Paige M. Bracci, PhD ² Lucie McCoy, MPH ¹ Lucas A. Salas, MD, PhD ⁴ Brock C. Christensen, PhD ^{4,5} Margaret Wrensch, PhD,¹ Karl T. Kelsey, MD ⁶ Jennie W. Taylor, MD ^{1,7} Jennifer L. Clarke, MD ^{1,7}

¹Department of Neurological Surgery, University of California San Francisco, San Francisco, CA, USA; ²Department of Epidemiology and Biostatistics, University of California San Francisco, San Francisco, CA, USA; ³Department of Biostatistics & Data Science, University of Kansas Medical Center, Kansas City, KS, USA; ⁴Department of Epidemiology, Geisel School of Medicine, Dartmouth College, Lebanon, NH, USA; ⁵Departments of Molecular and Systems Biology and Community and Family Medicine, Geisel School of Medicine, Dartmouth College, Lebanon, NH, USA; ⁶Departments of Epidemiology and Pathology and Laboratory Medicine, Brown University, Providence, RI, USA; and ⁷Department of Neurology, University of California San Francisco, San Francisco, CA, USA

*Correspondence to: Annette M. Molinaro, PhD, Department of Neurological Surgery, University of California San Francisco, 1450 3rd St, San Francisco, CA 94158 USA (e-mail: annette.molinaro@ucsf.edu).

Abstract

Background: Tumor-based classification of human glioma portends patient prognosis, but considerable unexplained survival variability remains. Host factors (eg, age) also strongly influence survival times, partly reflecting a compromised immune system. How blood epigenetic measures of immune characteristics and age augment molecular classifications in glioma survival has not been investigated. We assess the prognostic impact of immune cell fractions and epigenetic age in archived blood across glioma molecular subtypes for the first time. **Methods:** We evaluated immune cell fractions and epigenetic age in archived blood from the University of California San Francisco Adult Glioma Study, which included a training set of 197 patients with *IDH*-wild type, 1p19q intact, *TERT* wild type (*IDH*/1p19q/*TERT*-WT) glioma, an evaluation set of 350 patients with other subtypes of glioma, and 454 patients without glioma. **Results:** *IDH*/1p19q/*TERT*-WT patients had lower lymphocyte fractions ($CD4^+$ T, $CD8^+$ T, natural killer, and B cells) and higher neutrophil fractions than people without glioma. Recursive partitioning analysis delineated 4 statistically significantly different survival groups for patients with *IDH*/1p19q/*TERT*-WT based on an interaction between chronological age and 2 blood immune factors, $CD4^+$ T cells, and neutrophils. Median overall survival ranged from 0.76 years (95% confidence interval = 0.55-0.99) for the worst survival group ($n = 28$) to 9.72 years (95% confidence interval = 6.18 to not available) for the best ($n = 33$). The recursive partitioning analysis also statistically significantly delineated 4 risk groups in patients with other glioma subtypes. **Conclusions:** The delineation of different survival groups in the training and evaluation sets based on an interaction between chronological age and blood immune characteristics suggests that common host immune factors among different glioma types may affect survival. The ability of DNA methylation-based markers of immune status to capture diverse, clinically relevant information may facilitate noninvasive, personalized patient evaluation in the neuro-oncology clinic.

Identification of molecular subtypes of human glioma has helped refine these cancers' classification beyond traditional histopathologic and grade criteria (1-3). The current World Health Organization (WHO) 2016 glioma classification scheme incorporates tumor grade, isocitrate dehydrogenase (*IDH*1/2) mutational status, and 1p/19q co-deletion status (3). Glioblastomas (GBMs), the

most common type of glioma, are either *IDH*-mutant (9%) and occur at a median age of 38 years (with a median overall survival [OS] of 3.6 years) or are *IDH*-wild type (WT) (91%) and occur at a median age of 59 years (with a median OS of 1.2 years) (1,4). Non-GBM astrocytomas are either *IDH*-mutant and occur in younger patients (median age = 36 years), with a median OS of 9.3 years, or *IDH*-WT

Received: April 19, 2021; Revised: June 30, 2021; Accepted: September 23, 2021

© The Author(s) 2021. Published by Oxford University Press. All rights reserved. For permissions, please email: journals.permissions@oup.com

and occur in older patients (median age = 52 years), with a median OS of 1.9 years (1,4). Oligodendrogliomas have a median age of 44 years and a median OS of 17.5 years and are defined by both *IDH* mutation and co-deletion of 1 copy of the 1p and 19q chromosomal arms. Tumor telomerase promoter mutation (*TERT*) can further define subtypes (Molecular Subtypes 2015) (2,5). Up to 20% of patients with *IDH*-WT glioblastomas and 35% of those with *IDH*-WT astrocytomas lack 1p/19q co-deletion and *TERT* mutation (MT) (1); they are known as *IDH*/1p19q/*TERT*-WT gliomas, or “triple-negatives.” We previously showed that patients with *IDH*/1p19q/*TERT*-WT astrocytoma had statistically significantly longer and more variable survival than patients with *IDH*-WT/1p19q-WT/*TERT*-MT astrocytomas (4). The median OS was 3.3 years (95% confidence interval [CI] = 2.1 to not available [NA]) for patients with triple-negative astrocytoma vs 1.7 years (95% CI = 1.4 to 2.0) for those with *IDH*-WT/1p19q-WT/*TERT*-MT astrocytoma (4), which nonmolecular characteristics may further elucidate.

After the WHO 2016 classification, the single most important prognostic factor in adult glioma is age at diagnosis (6). Among patients with GBM, being older or younger than 50 years of age distinguishes shorter- and longer-term survival groups (7–11). Unknown mechanisms contribute to age as a dominant factor in glioma survival, but likely age-related immune system changes play a vital role (12). Most immune response components are affected during the aging process, which supports the concept of immunosenescence (13) and its corollary that a person’s immunologic “age” may diverge from their chronological age (14). Immune aging phenotypes include the diminished primary immune responses of older individuals and lower rates of successful vaccination (15) as well as age-related accumulation of memory effector T cells (16), deficits of naïve T cells (17), and central changes in bone marrow stem cell populations (18,19) leading to shifts in the balance of myeloid and lymphoid compartments. Thus, survival from glioma may depend on both patient age and specific immune characteristics. Measures of immune status that reflect individual immune aging may help disentangle the contribution of these interacting factors (20,21).

Both immune cell identification and understanding biological age have been areas of intensive epigenetic research that implicate the importance of DNA methylation. Immunomethylomics is an approach to immune cell profiling based on DNA methylation cytometry, which returns quantitative immune profile data using DNA methylation signatures specific for different immune cells (22–24). DNA-based immune profiling is reproducible; has a standardized workflow insensitive to batch and operator; and does not require intact cells, obviating the need for time-sensitive blood processing (which can include subjective gating procedures). Another line of epigenetic research has focused on DNA methylation-based epigenetic clocks as indicators of biological age (14). The initial blood-based models of Hannum (25) and the multitissue algorithm by Horvath (26) were trained to predict chronological age and, as such, strongly correlate with chronological age. Subsequently, more clinically relevant biomarkers of aging have been explored by replacing prediction of chronological age with the prediction of a surrogate measure of phenotypic age to differentiate morbidity and mortality risk among same-age individuals (27). One such novel epigenetic age metric, DNAmPhenoAge, is based on 513 CpG sites and is a statistically significant predictor of morbidity and mortality; it is also correlated with immune profiles signaling immunosenescence (27). Epigenetic age based on blood has not been examined in glioma survival, although 1 study assessed it in glioma tumor tissue (28).

Here, we integrated cutting-edge bioinformatic techniques to profile immune phenotype and epigenetic age using genome-scale DNA methylation measures. Our goal was to assess

whether noninvasive epigenetic measures, such as blood immune profiles and epigenetic age, and interactions of such measures with clinical variables delineate survival risk groups among *IDH*/1p19q/*TERT*-WT glioma patients and whether such risk group characterizations could be applied to other glioma subtypes.

Methods

Patient Samples

The San Francisco Adult Glioma Study (AGS) is a case-control study that includes 3164 patients newly diagnosed with glioma between 1991 and 2012 who were residents of the San Francisco Bay Area or patients of the University of California San Francisco (UCSF) neuro-oncology clinic and 2140 people without glioma who were residents of the San Francisco Bay Area or seen in the UCSF phlebotomy clinic (29). This study was approved by the institutional review board of the UCSF Human Research Protection Program in the Office of Ethics and Compliance under UCSF federal-wide assurance 00000068. Informed consent was obtained from all study participants.

The study population consisted of 2 independent sets of AGS patients with glioma (ie, the training and evaluation sets) plus a group of 454 AGS participants without glioma (Figure 1, A). Among patients with blood samples and molecular tumor marker data, methylation arrays were run for 197 patients with *IDH*/1p19q/*TERT*-WT (the training set) and 350 patients with other glioma subtypes (evaluation set: 41 *IDH*-MT gliomas [32 astrocytomas and 9 GBMs]; 130 *IDH*-WT gliomas [78 astrocytomas and 52 GBMs]; 141 patients with *IDH*-MT/1p19q co-deleted oligodendrogliomas; and 38 participants who could not be categorized according to WHO 2016) (Figure 1, A) (1,30). The 454 participants without glioma were partially matched to patients with *IDH*/1p19q/*TERT*-WT by age, sex, race, and AGS study phase. Blood samples were collected approximately 3 months after diagnosis.

DNA Methylation Array

Frozen anticoagulated whole blood was processed for DNA isolation and bisulfite conversion, as previously described (24). The Illumina 850K EPIC DNA methylation platform (Illumina, Inc, San Diego, CA) was used except for a subset of the evaluation set samples on the Illumina 450K array. Preprocessing and quality control of methylation array data are described in the [Supplementary Methods](#) (available online).

Immunomethylomic Assay

Using the preprocessed and normalized methylation data, we applied an optimized reference-based cell mixture deconvolution methodology (31) to the 3 cohorts to estimate the proportions of CD4⁺ T cells, CD8⁺ T cells, B cells, natural killer cells, monocytes, neutrophils, and 3 cell ratios (neutrophil-to-lymphocyte ratio [NLR], lymphocyte-to-monocyte ratio [LMR], and CD4⁺ T/CD8⁺ T cells).

Accuracy and reproducibility of cell deconvolution are previously described (23,24,32). A comparison of cell deconvolution using the 450K and 850K platforms run on the same 12-evaluation-set patients indicated close correspondence of cell proportion estimates across the 2 platforms ([Supplementary Figure 1](#), available online), and comparison of CD4⁺ T cell estimates by flow

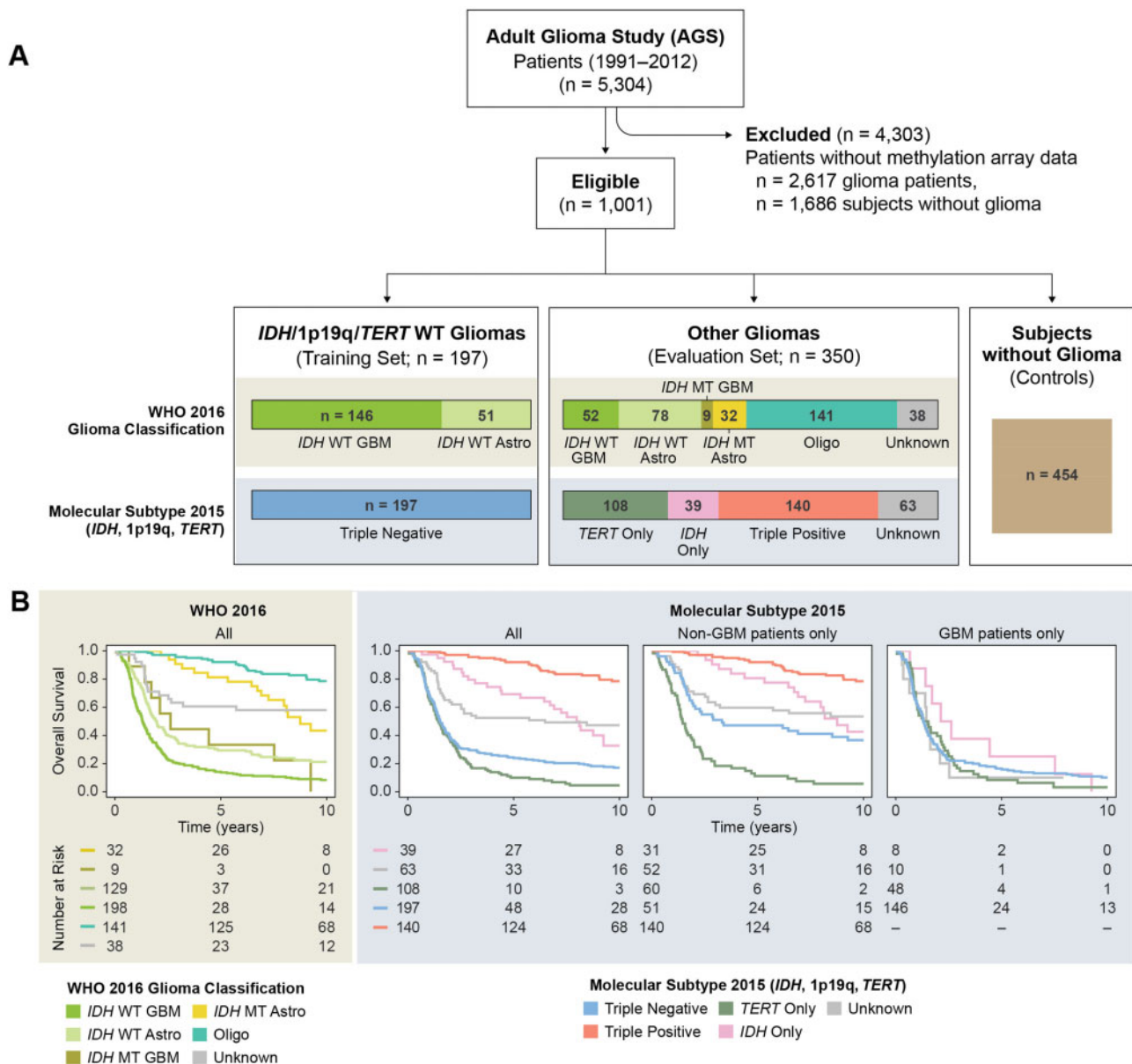


Figure 1. Adult Glioma Study (AGS) glioma cases and participants without glioma. **A)** Data flow diagram for the AGS participants, with World Health Organization (WHO) 2016 glioma classification and molecular subtypes 2015², for IDH/1p19q/TERT-wild type (WT) gliomas (training set) vs other glioma groups (evaluation set). **B)** Survival curves for the AGS glioma cases by WHO 2016 glioma classification and molecular subtypes 2015² classification. Astro = astrocytoma; GBM = glioblastoma; Oligo = oligodendroglioma.

cytometry vs cell deconvolution in 72 AGS patients illustrates their similarity (Supplementary Figure 2, available online).

DNAmAge, DNAmPhenoAge, and HannumAge Estimation

DNA methylation-based epigenetic clocks can be indicators of biological age (14). The 3 clocks evaluated were the initial blood-based models of Hannum (25) (HannumAge), a multitissue algorithm to predict chronological age (26) (DNAmAge), and a subsequent algorithm (27) to predict a surrogate measure of phenotypic age to differentiate morbidity and mortality risk among same-age individuals (DNAmPhenoAge).

Statistical Analysis

OS was defined as the time from the date of diagnosis until the date of death (ie, event) or date of last follow-up (ie, censored). Cox proportional hazards models were used to evaluate associations of overall patient survival with baseline clinical variables, immune profiles, and WHO 2016 glioma classification (Table 1). Because of violations of the linearity and proportional hazards assumptions and our primary goal to examine interactions, we assessed combinations of clinical and epigenetic markers via partDSA (33,34), a recursive partitioning algorithm that accommodates censored data (see the Supplementary Methods, available online, for details). We built models of increasing complexity in the training set: first,

Table 1. Demographic and clinical characteristics of patients in the adult glioma study: training set of 197 IDH/1p/19q/TERT wild type patients, evaluation set of 350 patients with another glioma, and 454 participants without glioma

Variable	Training IDH/1p19q/TERT WT patients (n = 197)	Evaluation set Patients with an- other glioma (n = 350)	Control participants without glioma (n = 454)	Training vs con- trols, P value	Training vs eval- uation, P value	Evaluation vs controls, P value
Clinical variables						
Chronological age, median (IQR), y	52.0 (41-64)	48.0 (40-56)	52.0 (41-63)	.91 ^a	.002 ^a	<.001 ^a
Days between diagnosis and blood draw, median (IQR)	103 (72-161)	104.5 (33-182)	—	—	.63 ^a	—
Sex, No. (%)				.20 ^b	.71 ^b	.27 ^b
Female	79 (40.1)	146 (41.7)	207 (45.6)			
Male	118 (59.9)	204 (58.3)	247 (54.4)			
Smoking status, No. (%)				<.001 ^b	.19 ^b	.001 ^b
Missing	0	2	1			
Current	26 (13.2)	35 (10.1)	61 (13.5)			
Ever/past	84 (42.6)	126 (36.2)	164 (36.2)			
Never	87 (44.2)	187 (53.7)	228 (50.3)			
Alcohol drinking status, No. (%)				<.001 ^b	.003 ^b	<.001 ^b
Missing	0	2	1			
Current	116 (58.9)	169 (48.6)	226 (49.9)			
Ever/past	65 (33.0)	152 (43.7)	160 (35.4)			
Never	16 (8.1)	27 (7.8)	67 (14.8)			
BMI, median (IQR), kg/m ²	25.7 (23.3-29.1)	26.1 (23.2-29.5)	25.8 (23.3-29.8)	.16 ^a	.41 ^a	.44 ^a
Race, No. (%)				.06 ^b	.02 ^b	<.001 ^a
Asian	18 (9.1)	20 (5.7)	32 (7.0)			
Black	7 (3.6)	1 (0.3)	50 (11.0)			
Native American	1 (0.5)	1 (0.3)	2 (0.4)			
Other	9 (4.6)	11 (3.1)	17 (3.7)			
Pacific Islander	0 (0.0)	1 (0.3)	1 (0.2)			
White	162 (82.2)	316 (90.3)	352 (77.5)			
Vital status, No. (%)				—	<.001 ^b	—
Alive	28 (14.2)	145 (41.4)	—			
Dead	169 (85.8)	205 (58.6)	—			
Follow-up, median (95% CI), y	15 (12.9 to 19.0)	12.3 (10.6 to 13.7)	—	—	<.001 ^b	—
WHO 2016 Glioma Classification, No. (%)				—	<.001 ^b	—
Missing	0	38	—			
IDH-WT glioblastoma	146 (74.1)	52 (16.7)	—			
IDH-WT astrocytoma	51 (25.9)	78 (25.0)	—			
IDH mutant glioblastoma	0 (0.0)	9 (2.9)	—			
IDH mutant astrocytoma	0 (0.0)	32 (10.3)	—			
IDH mutant/1p19q co-deleted oligodendroglioma	0 (0.0)	141 (45.2)	—			
Glioma diagnosis grade, No. (%)				—	<.001 ^b	—
Missing	0	1	—			
Grade 2	18 (9.1)	163 (46.7)	—			
Grade 3	33 (16.8)	120 (34.4)	—			
Grade 4	146 (74.1)	66 (18.9)	—			
Molecular subtype (based on IDH, 1p19q, and TERT) ^{c*} , No. (%)				—	<.001 ^b	—
Missing	0 (0.0)	63 (18.0)	—			
IDH only	0 (0.0)	39 (11.1)	—			
TERT only	0 (0.0)	108 (30.9)	—			
Triple negative	197 (100.0)	0 (0.0)	—			
Triple positive	0 (0.0)	140 (40.0)	—			
Surgery, No. (%)				—	.48 ^b	—
Biopsy only	26 (13.2)	39 (11.1)	—			
Surgery	171 (86.8)	311 (88.9)	—			
Chemotherapy, No. (%)				—	.001 ^b	—
Missing	0	3	—			
No	41 (20.8)	117 (33.7)	—			
Yes	156 (79.2)	230 (66.3)	—			

(continued)

Table 1. (continued)

Variable	Training IDH/1p19q/TERT WT patients (n = 197)	Evaluation set Patients with an- other glioma (n = 350)	Control participants without glioma (n = 454)	Training vs con- trols, P value	Training vs eval- uation, P value	Evaluation vs controls, P value
Radiation, No. (%)				—	<.001 ^b	—
No	15 (7.6)	141 (40.3)	—			
Yes	182 (92.4)	209 (59.7)	—			
Treatment, No. (%)				—	<.001 ^b	—
Missing	0	3	—			
Both chemotherapy and radiation	152 (77.2)	160 (46.1)	—			
Chemotherapy only	4 (2.0)	70 (20.2)	—			
Radiation only	30 (15.2)	47 (13.5)	—			
Neither	11 (5.6)	70 (20.2)	—			
Taking dexamethasone at blood draw, No. (%)				<.001 ^b	<.001 ^b	<.001 ^b
Missing	1	6	6			
No	97 (49.5)	229 (66.6)	447 (99.8)			
Yes	99 (50.5)	115 (33.4)	1 (0.2)			
Epigenetic age variable						
DNAmAge, median (IQR), y	57.4 (47.0-66.0)	54.8 (46.6-63.0)	56.7 (44.9-66.4)	.51 ^a	.17 ^a	.46 ^a
DNAmPhenoAge, median (IQR), y	48.7 (36.9-58.1)	42.9 (34.0-51.8)	43.3 (31.5-54.9)	<.001 ^a	<.001 ^a	.55 ^a
HannumAge, median (IQR), y	45.8 (35.9-53.7)	45.0 (35.5-53.2)	42.9 (32.9-52.7)	.04 ^a	.44 ^a	.10 ^a
DNAmPhenoAge acceleration with IPs, median (IQR), y	-0.3 (-3.1-3.7)	-0.9 (-3.5 to 3.1)	-0.0 (-3.6 to 3.7)	.37 ^a	.08 ^a	.32 ^a
DNAmPhenoAge acceleration without IPs, median (IQR), y	2.6 (-1.8 to 6.5)	0.8 (-3.0 to 5.1)	-2.0 (-6.4 to 2.4)	<.001 ^a	.003 ^a	<.001 ^a
HannumAge acceleration with IPs, median (IQR), y	-1.0 (-4.2 to 1.3)	0.3 (-2.4 to 3.2)	0.1 (-2.6 to 2.5)	.003 ^a	<.001 ^a	.09 ^a
HannumAge acceleration without IPs, median (IQR), y	0.4 (-2.4 to 2.5)	1.5 (-1.8 to 5.9)	-2.1 (-4.8 to 0.4)	<.001 ^a	<.001 ^a	<.001 ^a
DNAmAge acceleration with IPs, median (IQR), y	-1.1 (-3.7 to 1.9)	1.0 (-2.4 to 4.1)	-0.6 (-3.7 to 2.8)	.89 ^a	.002 ^a	<.001 ^a
DNAmAge acceleration with- out IPs, median (IQR), y	-0.8 (-3.5 to 1.9)	1.3 (-1.8 to 4.8)	-1.4 (-4.2 to 2.2)	.15 ^a	<.001 ^a	<.001 ^a
IP variable						
B cell, median (IQR)	2.1 (1.3-3.4)	3.3 (2.0-4.9)	5.3 (4.0-7.0)	<.001 ^a	<.001 ^a	<.001 ^a
Monocyte, median (IQR)	7.5 (6.0-9.5)	7.7 (5.9-10.0)	7.4 (6.0-9.4)	.28 ^a	.74 ^a	.07 ^a
Neutrophils, median (IQR)	70.4 (61.7-80.5)	64.5 (55.4-71.9)	57.9 (51.0-65.5)	<.001 ^a	<.001 ^a	<.001 ^a
NK, median (IQR)	2.9 (1.9-4.5)	3.3 (1.9-5.1)	4.7 (3.4-6.2)	<.001 ^a	.37 ^a	<.001 ^a
CD4-positive T, median (IQR)	8.9 (5.2-14.2)	12.5 (8.2-17.8)	15.7 (11.8-19.7)	<.001 ^a	<.001 ^a	<.001 ^a
CD8-positive T, median (IQR)	6.3 (3.4-9.6)	7.3 (4.4-11.4)	8.9 (6.1-12.6)	<.001 ^a	.002 ^a	<.001 ^a
CD4-positive T/CD8-positive T, median (IQR)	1.5 (0.9-2.6)	1.6 (1.1-2.4)	1.7 (1.2-2.6)	.16 ^a	.08 ^a	.19 ^a
LMR, median (IQR)	2.8 (1.9-4.2)	3.8 (2.3-5.3)	4.8 (3.8-6.4)	<.001 ^a	<.001 ^a	<.001 ^a
NLR, median (IQR)	3.2 (2.0-5.9)	2.3 (1.4-3.7)	1.6 (1.2-2.2)	<.001 ^a	.002 ^a	<.001 ^a
Total lymphocytes, median (IQR)	21.3 (13.8-30.6)	28.3 (19.7-37.8)	37.1 (29.4-43.9)	<.001 ^a	<.001 ^a	<.001 ^a

^aLinear model ANOVA. All tests were 2-sided. ANOVA = analysis of variance; BMI = body mass index; CI = confidence interval; IP = immune profile; IQR = interquartile range; LMR = lymphocyte-to-monocyte ratio; NK = natural killer; NLR = neutrophil-to-lymphocyte ratio; WHO = World Health Organization; WT = wild type.

^bPearson χ^2 test. All tests were 2-sided.

^cPatients were categorized into 5 glioma groups based on 3 tumor molecular markers: IDH, 1p19q, and TERT. Details of how these were categorized can be found in Eckel-Passow et al. (2).

Clinical Variables Only; then, Clinical and Immune Profiles; finally, Clinical, Immune Profiles, and Epigenetic Ages. Subsequently, the risk groups' generalizability was assessed by the evaluation set—see the [Supplementary Methods](#) (available online) for details. For training and evaluation sets,

within- and between-group summary measures were based on the restricted mean survival time (RMST), which does not require the proportional hazards assumption (35). Two-sided tests of statistical significance were used, and $P < .05$ was selected as the cutoff for statistical significance. All analyses

were performed in R, version 4.0.2 (R Foundation for Statistical Computing, Vienna, Austria) (36).

Results

Clinical and Demographic Characteristics of Patients With Glioma and Controls

Figure 1 shows the 3 sets of participants and molecular classifications for patients with glioma. Clinical and demographic characteristics are in Table 1. Because of frequency matching for choosing participants without glioma, age, race, and sex were similar to those of *IDH/1p19q/TERT*-WT glioma patients. Fewer participants without glioma than *IDH/1p19q/TERT*-WT glioma patients consumed alcohol, smoked, or took dexamethasone at blood draw. Evaluation set patients were younger, less likely to consume alcohol at blood draw, predominantly White, less likely to receive chemotherapy or radiation, and less likely to be on dexamethasone than the training set patients. Compared with the participants without glioma, the other patients with glioma were younger, less likely to be current smokers, more likely to have consumed alcohol, and more likely to be White.

Blood Immune Profiles Alterations in *IDH/1p19q/TERT*-WT Patients

The *IDH/1p19q/TERT*-WT patients had increased fractions of neutrophils and lower proportions of B cells, $CD4^+$ T, $CD8^+$ T, natural killer cells, and total lymphocytes compared with participants without glioma (all $P < .001$; Figure 2 and Table 1). The NLR was higher among *IDH/1p19q/TERT*-WT patients compared with participants without glioma (median [interquartile range (IQR)] = 3.2 [2.0-5.9] vs 1.6 [1.2-2.2], $P < .001$), while LMR was lower (median [IQR] = 2.8 [1.9-4.2] vs 4.8 [3.8-6.4], $P < .001$), and the $CD4^+$ T-to- $CD8^+$ T cell ratio was not statistically significantly different (median [IQR] = 1.5 [0.9-2.6] vs 1.7 [1.2-2.6], $P = .16$).

There were consistent differences in leukocyte proportions for grade 4 vs grade 2 to 3 *IDH/1p19q/TERT*-WT tumors (Supplementary Table 1, available online). Further stratification of the 196 *IDH/1p19q/TERT*-WT patients with dexamethasone status known at blood draw revealed a greater neutrophil proportion; higher NLR; and lower $CD4^+$ T, $CD8^+$ T, natural killer-cell, and B-cell proportions among dexamethasone-exposed vs nonexposed patients (Supplementary Table 2, available online). Similar relationships were seen in the other patients with glioma (Supplementary Tables 3 and 4, available online).

The *IDH/1p19q/TERT*-WT patients also had an increased fraction of neutrophils and higher NLR than the other patients with glioma and decreased B cells, $CD4^+$ T cells, $CD8^+$ T cells, total lymphocytes, and LMR (Table 1). The distributions of immune profiles were statistically different between the other patients with glioma and the participants without glioma, except for monocytes (Table 1).

Correlations Between Epigenetic Age and Immune Profiles in *IDH/1p19q/TERT*-WT Patients and Participants Without Glioma

Among the 3 DNA methylation age estimates, DNAmPhenoAge and HannumAge were higher in patients with *IDH/1p19q/TERT*-

WT than in participants without glioma (Table 1). The DNAmPhenoAge and HannumAge age acceleration were also increased. Once adjusted for leukocyte cell type composition, only HannumAge age acceleration remained statistically significant (median [IQR] = -1.0 [-4.2 to 1.3] vs 0.1 [-2.6 to 2.5], $P = .003$). Both in *IDH/1p19q/TERT*-WT patients and in participants without glioma, chronological age was modestly negatively correlated with lymphocyte subsets and positively associated with neutrophils (Supplementary Figure 3, available online). Stronger associations were observed for the HannumAge and DNAmPhenoAge measures.

Survival in *IDH/1p19q/TERT*-WT Patients and Variations in Blood Immune Profiles

The median OS for the 197 *IDH/1p19q/TERT*-WT patients was 1.5 years (95% CI = 1.4 to 1.8) (Figure 1, B and Supplementary Table 5, available online). Split by the WHO 2016 classification, the *IDH*-wildtype GBMs had a median OS of 1.3 years (95% CI = 1.2 to 1.52), and the *IDH*-WT astrocytomas had 3.3 years (95% CI = 1.97 to NA). Univariate survival models are in Figure 3, A and Supplementary Table 6 (available online).

Clinical Variables Only. Interactions were explored by constructing survival recursive partitioning analyses (RPAs), including univariately statistically significant clinical variables (Figure 3, B). Important interactions among age, dexamethasone use, and body mass index (BMI) were elucidated and separated the patients into 4 mutually exclusive risk groups (Supplementary Figure 4, A, available online). The patients with the best survival were younger, not taking dexamethasone, and had a lower BMI (group 1, gold: $n = 34$, median OS = 9.19 years [95% CI = 6.18 to NA]). The second-best survival risk group included the younger patients not taking dexamethasone but with higher BMI (group 2, tan: $n = 26$, median OS = 3.33 years [95% CI = 1.74 to NA]). The second-worst survival group included 2 subgroups: younger patients taking dexamethasone and older patients with a low BMI (group 3, gray: $n = 89$, median OS = 1.47 years [95% CI = 1.31 to 1.69]). The patients who had the worst survival were older, with a higher BMI (group 4, blue: $n = 47$, median OS = 0.78 years [95% CI = 0.67 to 0.99]). RMST estimates for the group assignment are given in Table 2 (Model A: Clinical Variables).

Clinical Variables and Immune Profiles. We then added immune profile variables to the clinical variables (Figure 3, B). Interactions among age, $CD4^+$ T cell, and neutrophil proportions separated the patients into 4 mutually exclusive survival groups (Figure 4, A). The patients with the best survival were younger, with a high $CD4^+$ T-cell proportion (group 1, gold: $n = 33$; median OS = 9.72 years [95% CI = 6.18 to NA]). The second-best survival risk group included young patients with a low $CD4^+$ T-cell proportion (group 2, tan: $n = 93$; median OS = 1.75 years [95% CI = 1.50 to 2.06]). The second-worst survival was experienced by those who were older and had a low neutrophil proportion (group 3, gray: $n = 43$, median OS = 1.27 years [95% CI = 0.83 to 1.64]). The patients who had the worst survival included those who were older and had high neutrophil proportions (group 4, blue: $n = 28$, median OS = 0.76 years [95% CI = 0.55 to 0.99]). Kaplan-Meier survival curves show the discrimination of survival groups (Figure 4, B). *IDH*-WT GBM comprises 96.4% of group 4, 81.4% of group 3, 74.2% of group 2, and 45.5% of group 1 (Figure 4, A; Supplementary Table 7, available online). Kaplan-Meier curves are in Figure 4, B, and RMST estimates are in Table 2 (Model B: Clinical + Immune Profiles). Blood draw

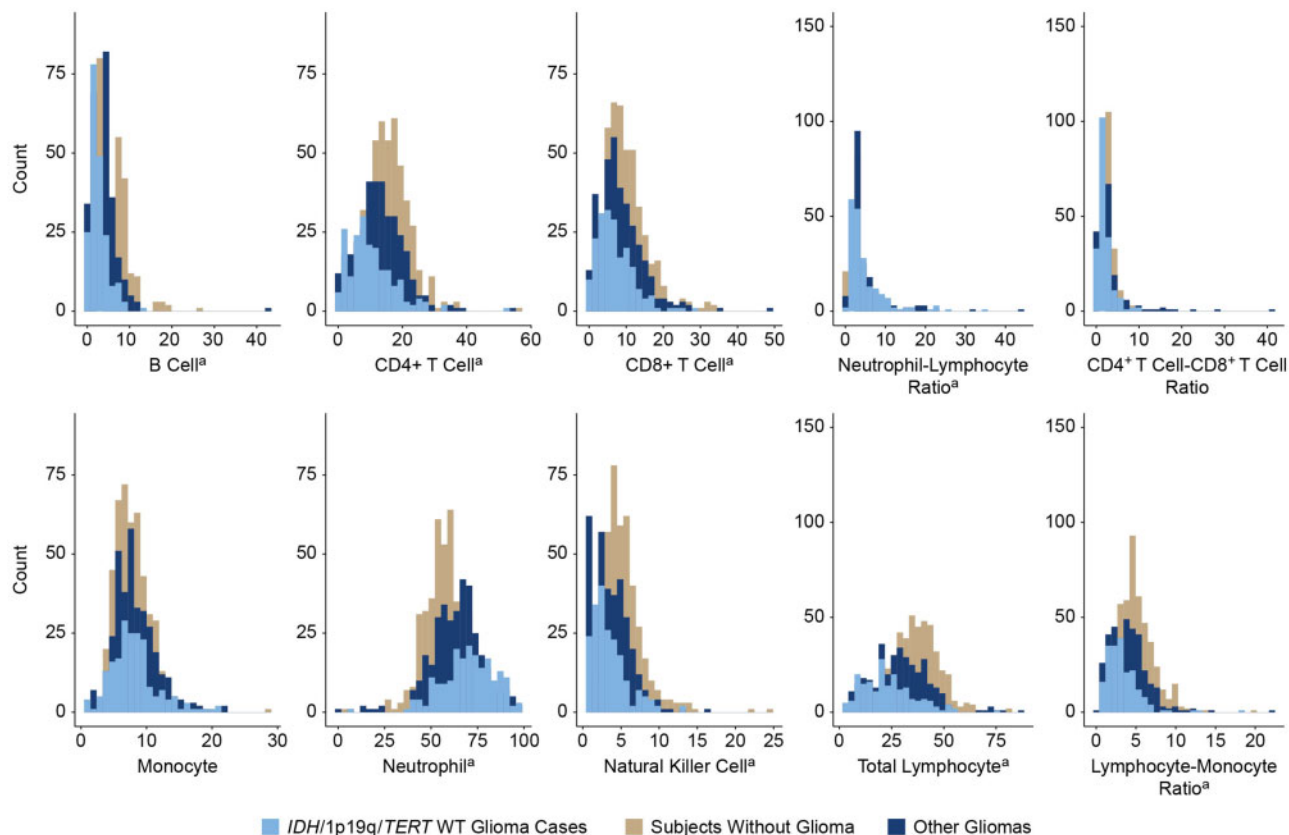


Figure 2. Comparisons of immune cell fractions in blood from the training set of 197 *IDH1/1p19q/TERT*-wild type (WT) patients, evaluation set of 350 other glioma groups, and 454 participants without glioma.

^aIndicates a statistically significant difference in the specified immune cell fractions via analysis of variance.

treatment time points were included in the survival RPA, but this variable did not statistically significantly affect the survival results (Supplementary Table 8, available online).

Clinical Variables, Immune Profiles, and Epigenetic Ages. Next, we included HannumAge and DNAmPhenoAge and the clinical and immune profile data (Figure 3, B). Important interactions among HannumAge, CD4⁺ T cells, and neutrophil proportions were identified (Supplementary Figure 5, A, available online). Patients fell into 1 of 4 risk groups. The patients with the best survival had a younger HannumAge and a high CD4⁺ T-cell proportion (group 1, gold: n=31, median OS=14.0 years [95% CI=8.33 to NA]). The second-best survival risk group included younger HannumAge, with a low CD4⁺ T-cell proportion (group 2, tan: n=77, median OS=1.97 years [95% CI=1.54 to 2.91]). The second-worst survival was experienced by those who were older by HannumAge and had a lower neutrophil proportion (group 3, gray: n=52, median OS=1.27 years [95% CI=0.89 to 1.69]). The older patients by HannumAge who had a higher neutrophil proportion had the worst survival (group 4, blue: n=37, median OS=0.79 years [95% CI=0.63 to 0.99]). Kaplan-Meier curves are shown in Supplementary Figure 5, B (available online), and RMST estimates are in Table 2 (Model C: Clinical + Immune Profiles + HannumAge). An interaction between DNAmPhenoAge and years of education was identified (Supplementary Figure 6, A, available online). Kaplan-Meier curves are shown in Supplementary Figure 6, B (available online) and RMST estimates are in Table 2 (Model C: Clinical + Immune Profiles + DNAmPhenoAge).

Survival Among Other Patients With Glioma. The 350 other patients with glioma had a median OS of 7.5 years (95% CI=6.1 to 10.6). Survival by WHO 2016 and Molecular Subtype 2015 guidelines are shown in Figure 1, B and Supplementary Table 5 (available online). We assessed whether the same variables and cut points built by the 4 RPA models also distinguished survival among the other glioma cases. Only the RPA from the Clinical Variable and Immune Profiles (Figure 4, C and D) distinguished 4 survival groups based on the same cut points generated by the training set, whereas in the other 3, 2 of the 4 groups collapsed (Supplementary Figures 4, C; 5, C; and 6, C, available online; Table 2). The Kaplan-Meier curves in Figure 4, D, estimate the median OS for group 4 as 0.7 years (95% CI=0.4 to 1.4), for group 3 as 2.5 years (95% CI=1.6 to 5.7), for group 2 as 8.2 years (95% CI=6.2 to NA), and for group 1 as 13.6 years (95% CI=10.6 to 18.2). The RMST estimates are in Table 2. Oligodendrogliomas comprise 0% of group 4, 30.8% of group 3, 35.9% of group 2, and 56.1% of group 1 (Figure 4, C; Supplementary Table 9, available online). Groups by Molecular Subtype 2015 are in Supplementary Figure 7 and Supplementary Table 9 (available online).

Discussion

In this study, we explored the utility of blood DNA methylation-based measures of age and immune cells to create prognostic patient subgroups that may augment traditional WHO classification. Consistent with past studies in the *IDH*-WT gliomas, age at diagnosis (chronological or epigenetic) figured prominently in

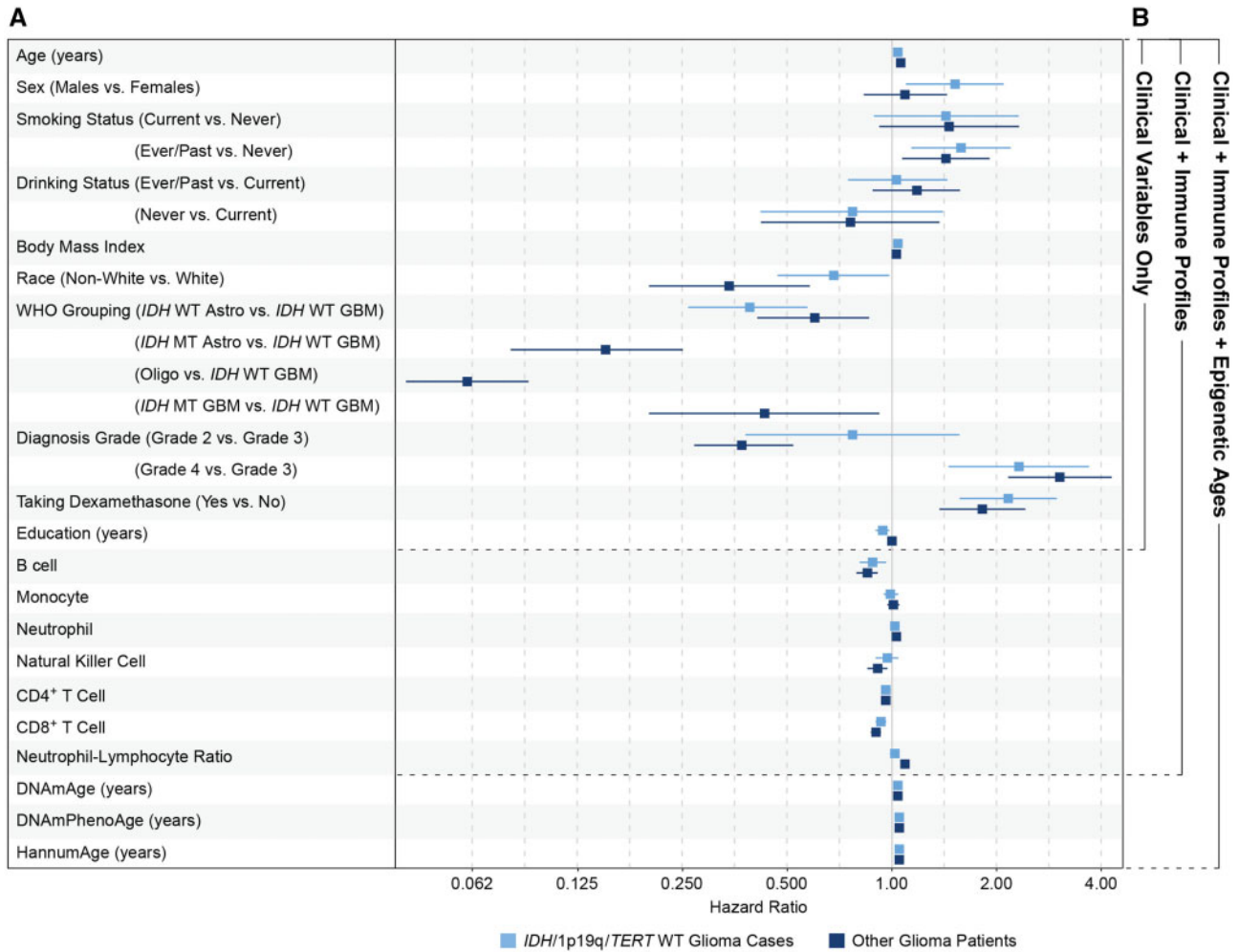


Figure 3. Forest plot of hazard ratios for univariate survival models and recursive partitioning analysis (RPA) model inclusion. **A)** The hazard ratios (squares) and 95% confidence intervals (error bars) for the training set of 197 *IDH/1p19q/TERT*-wild type (WT) gliomas in light blue and the 350 other glioma groups in dark blue. For the *IDH/1p19q/TERT*-WT gliomas, violations of the proportional hazards assumption occurred in the univariate models for chronological age, monocytes, DNAmAge, DNAmPhenoAge, and HannumAge. For the other gliomas, violations of the proportional hazards assumption occurred in the univariate models for chronological age, World Health Organization (WHO) grouping, diagnosis grade, taking dexamethasone, monocytes, neutrophils, natural killer cells, CD4-positive T cells, CD8-positive T cells, DNAmAge, DNAmPhenoAge, and HannumAge. **B)** Variable groupings depict which variables are included in each of the 3 RPA models: clinical variables only; clinical variables + immune profiles (IPs); clinical variables, IPs, and epigenetic ages. Astro = astrocytoma; GBM = glioblastoma; Oligo = oligodendroglioma.

survival models (11). Although strongly correlated with chronological age, epigenetic-based age algorithms are designed to represent multisystem proxies of physiologic dysregulation. Such markers could convey patient-specific information about disease outcomes, but these epigenetic age measures were not consistently informative for glioma survival because neither the HannumAge nor the DNAmPhenoAge RPAs generalized to the other glioma patients. Nonetheless, in these models, immune cell proportions were associated with survival. Given the correlation between immune cell proportions and epigenetic age, epigenetic age appears to be a proxy of immune status, the latter being better captured by the immune cell proportions themselves.

Specifically, we showed that proportions of CD4 T cells and neutrophils and patient chronological age divided both sets of patients into 4 groups with statistically significantly different survival experiences. In both the training and evaluation sets, younger patients (aged ≤ 58 years) with higher CD4⁺ T-cell proportions and older patients (aged > 58 years) with lower neutrophil proportions both had better survival. The reciprocal

increase in myeloid cells and decreased lymphocytes associated with worse survival are a recurring theme in many cancers (37).

Although the same factors distinguished survival in the 2 independent sets of patients, the groups' median survival times were different, reflecting the different underlying survival of participants according to glioma subtype. Interestingly, because of the inclusion of subgroups with better survival, there were somewhat greater differences in the survival times of the patients in the evaluation set than in the training set. Notably, among the *IDH/1p19q/TERT*-WT patients, although a large majority of the older patients with high neutrophils (ie, the highest-risk group), were *IDH*-WT GBM, as expected; almost half of the lowest risk group (ie, the younger patients with high CD4⁺ T cells) were also *IDH*-WT GBM. Similarly, in the other patients with glioma, although just over half of the lowest-risk group had oligodendrogliomas, one-third of the third-highest risk group (ie, the older patients with lower neutrophil proportion) also had oligodendrogliomas. Finally, patients whose tumors could not be assigned to a WHO subtype still were distributed across each of the 4 risk groups. Therefore, an

Table 2 Recursive partitioning analysis models: training set of 197 *IDH1/1p19q/TERT* wild type patients and evaluation set of 350 patients with another glioma from the adult glioma study

Model description	Group ^a	Training set (n = 197)		Evaluation set (n = 350)	
		RMST (95% CI)	P value ^b	RMST (95% CI)	P value ^b
Model A: clinical variables ^c	Clinical-only tree				
	Best survival (group 1, gold)	9.14 (7.17 to 11.12)	.12	10.36 (9.12 to 11.61)	.68
	Second-best survival (group 2, tan)	6.66 (4.26 to 9.07)	(Referent)	10.01 (8.89 to 11.13)	(Referent)
	Second-worst survival (group 3, gray)	2.86 (2.08 to 3.65)	.003	6.82 (5.70 to 7.94)	<.001
	Worst survival (group 4, blue)	1.40 (0.76 to 2.05)	<.001	3.91 (2.51 to 5.30)	<.001
Model B: clinical + IPs ^d	Clinical + IPs tree				
	Best survival (group 1, gold)	9.33 (7.32 to 11.34)	<.001	10.09 (9.08 to 11.11)	.03
	Second-best survival (group 2, tan)	4.07 (3.08 to 5.07)	(Referent)	8.50 (7.53 to 9.48)	(Referent)
	Second-worst survival (group 3, gray)	2.07 (1.16 to 2.98)	.004	5.18 (3.68 to 6.68)	<.001
	Worst survival (group 4, blue)	1.15 (0.36 to 1.95)	<.001	0.83 (0.54 to 1.12)	<.001
Model C: clinical + IPs + HannumAge ^e	Clinical + IPs + HannumAge tree				
	Best survival (group 1, gold)	9.74 (7.68 to 11.80)	<.001	10.18 (9.10 to 11.27)	.90
	Second-best survival (group 2, tan)	4.69 (3.54 to 5.85)	(Referent)	10.08 (8.87 to 11.30)	(Referent)
	Second-worst survival (group 3, gray)	1.98 (1.22 to 2.73)	<.001	6.44 (5.32 to 7.56)	<.001
	Worst survival (group 4, blue)	1.13 (0.52 to 1.73)	<.001	2.66 (1.63 to 3.69)	<.001
Model D: clinical + IPs + DNAmPhenoAge ^f	Clinical + IPs + DNAmPhenoAge tree				
	Best survival (group 1, gold)	8.07 (6.50 to 9.64)	<.001	10.65 (9.73 to 11.58)	<.001
	Second-best survival (group 2, tan)	3.58 (2.54 to 4.63)	(Referent)	6.72 (5.66 to 7.78)	(Referent)
	Second-worst survival (group 3, gray)	1.64 (0.96 to 2.33)	.003	6.98 (5.50 to 8.46)	.78
	Worst survival (group 4, blue)	1.29 (0.30 to 2.28)	.002	2.80 (0.99 to 4.61)	.002

^aModel A: Group 1 (gold) were ≤ 58 years of age, were not taking dexamethasone at the time of blood draw, and had a BMI ≤ 26 kg/m². Group 2 (tan) were ≤ 58 years of age, were not taking dexamethasone at the time of blood draw, and had a BMI > 26 kg/m². Group 3 (gray) were either > 58 years of age and had a BMI ≤ 24 kg/m² or were ≤ 58 years of age and took dexamethasone at the time of blood draw. Group 4 (blue) were > 58 years of age and had a BMI > 24 kg/m². Model B: Group 1 (gold) were ≤ 58 years of age and had a CD4-positive T-cell count > 14 . Group 2 (tan) were ≤ 58 years of age and had CD4-positive T-cell count ≤ 14 . Group 3 (gray) were > 58 years of age and had a neutrophil count ≤ 77 . Group 4 (blue) were > 58 years of age and had a neutrophil count > 77 . Model C: Group 1 (gold) consisted of the 31 patients who were ≤ 47 years of age by HannumAge and had CD4-positive T-cell count > 14 . Group 2 (tan) were ≤ 47 years of age by HannumAge and had CD4-positive T-cell count ≤ 14 . Group 3 (gray) were > 47 years of age by HannumAge and had a neutrophil count ≤ 74 . Group 4 (blue) were > 47 years of age by HannumAge and had a neutrophil count > 74 . Model D: Group 1 (gold) were ≤ 39.5 years of age by DNAmPhenoAge. Group 2 (tan) were between 39.5 and 63.2 years of age by DNAmPhenoAge and had > 15 years of education. Group 3 (gray) were between 39.5 and 63.2 years of age by DNAmPhenoAge and had ≤ 15 years of education. Group 4 (blue) were > 63.2 years of age by DNAmPhenoAge. BMI = body mass index; CI = confidence interval; IP = immune profile; RMST = restricted mean survival time; RPA = recursive partitioning analysis.

^bTwo-sided P values were calculated using the Wald test.

^cRMST for RPA in [Supplementary Figure 4, A](#) (available online).

^dRMST for RPA in [Figure 4, A](#).

^eRMST for RPA in [Supplementary Figure 5, A](#) (available online).

^fRMST for RPA in [Supplementary Figure 6, A](#) (available online).

interaction between chronological age and immune cell composition may fine-tune the current prognostic molecular classification systems and, if validated in other studies, may be critical when molecular data are insufficient for classification.

One of this study's limitations was that blood samples were obtained after diagnostic surgery (on average within 3 months of diagnosis), not at uniform times relative to other treatments. Blood draw timing did not affect our analyses' outcome ([Supplementary Table 8](#), available online). Other limitations are that the 6 immune factors are cell proportions rather than absolute cell counts and do not capture additional subtypes. Finally, we had incomplete data on some tumor markers, such as EGFR, TP53, CDKN2A/B, and MGMT, but our evaluation set of patients with glioma represented the various WHO 2016 glioma subtypes not represented in the training set. We also acknowledge that some of the variability in the survival data could have been the result of potential diagnostic misclassification despite the use of several relevant tumor markers. For example, studies have shown that classification by tumor methylation arrays can change diagnoses in up to 12% of patients with glioma and is becoming a more standard diagnostic approach where available

(38). It will be many years, however, until cohorts of patients with glioma diagnosed using today's methylation arrays or other, new diagnostic paradigms have sufficient events for rigorous outcomes studies. Thus, the use of the available markers on this historic, well-characterized cohort is of value now and in future glioma research.

Abnormalities in peripheral blood immune profiles have long been observed in patients with glioma (39-42) and associated with glioma outcomes (30,43). The current studies illustrate how peripheral blood is a rich source of immune biomarker information, reflecting the dynamic interactions of tumor and host and the beneficial or deleterious effects of therapeutic interventions (44,45). The critical impact of the systemic immune compartment on antitumor immunity has been highlighted in recent studies of checkpoint inhibition therapy in animal models (46) and humans (47-49). These observations' potential relevance for patients with GBM was illustrated in a recent neoadjuvant programmed death-ligand 1 blockade trial that found response rates linked with pretherapy (baseline) blood immune profiles (50). DNA methylation has significant potential to contribute to these efforts and provide noninvasive

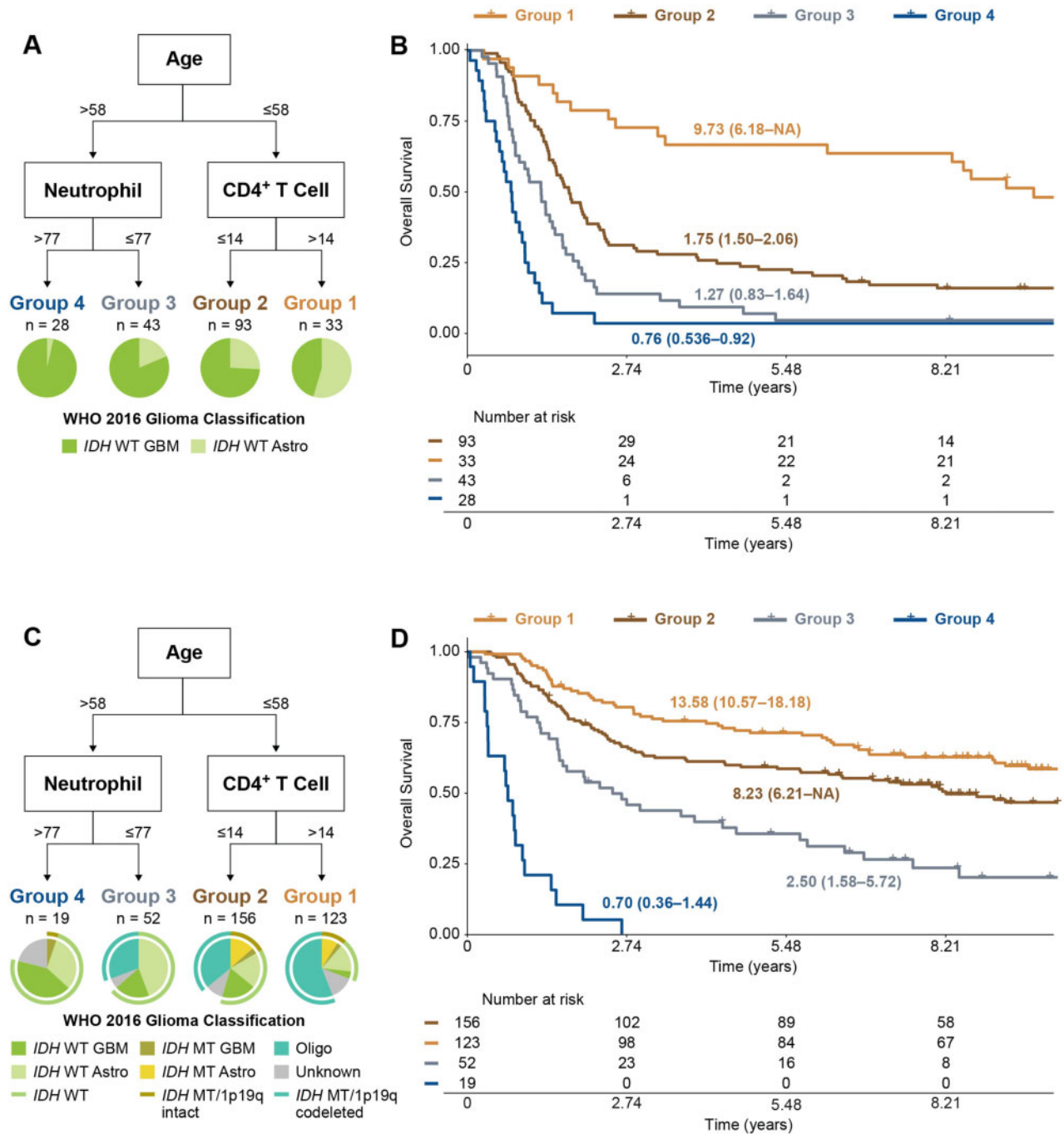


Figure 4. Clinical + immune profiles recursive partitioning analysis (RPA), and Kaplan-Meier curves in the training and evaluation sets. **A)** For the clinical + IPs RPA in the training set of 197 IDH/1p19q/TERT-wild type (WT) patients, chronological age was the RPA’s primary node, with neutrophil counts and CD4 T-cell counts as secondary nodes. Patients fell into 1 of 4 risk groups: Group 1 (gold) consisted of the 33 patients who were ≤58 years of age and had CD4 T-cell counts >14, with a median overall survival (OS) of 9.73 years (95% confidence interval [CI] = 6.18 to NA). Group 2 (tan) consisted of the 93 patients who were ≤58 years of age and had CD4-positive T-cell counts ≤14, with a median OS of 1.75 years (95% CI = 1.50 to 2.06). Group 3 (gray) consisted of the 43 patients who were >58 years of age and had a neutrophil count ≤77, with a median OS of 1.27 years (95% CI = 0.83 to 1.64). Group 4 (blue) consisted of the 28 patients >58 years of age with a neutrophil count >77 and a median OS of 0.76 years (95% CI = 0.55 to 0.99). World Health Organization (WHO) 2016 glioma classifications for 4 groups are shown in pie charts. **B)** Kaplan-Meier curves are shown for the training set based on the clinical + IPs RPA. Kaplan-Meier curves and risk table in the training set of 197 IDH/1p19q/TERT-WT patients for risk groups 1-4 are defined in Figure 4, A. **C)** The evaluation set of 350 patients with another glioma for risk groups 1-4 are defined by the training set RPA in Figure 4, A. Evaluation set patients fell into 1 of 4 risk groups defined by the training set. Group 1 (gold) consisted of the 123 patients who were ≤58 years of age and had CD4 T-cell count >14, with a median OS of 13.58 years (95% CI = 10.57 to 18.18). Group 2 (tan) consisted of the 156 patients who were ≤58 years of age and had a CD4 T-cell count ≤14, with a median OS of 8.26 years (95% CI = 6.21 to NA). Group 3 (gray) consisted of the 52 patients who were >58 years of age and had a neutrophil count ≤77, with a median OS of 2.496 years (95% CI = 1.58 to 5.72). Group 4 (blue) consisted of the 19 patients >58 years of age, with a neutrophil count >77 and a median OS of 0.70 years (95% CI = 0.36 to 1.44). WHO 2016 glioma classifications for the 4 groups are shown in pie charts. **D)** Kaplan-Meier curves are shown for the evaluation set based on the training set clinical + IPs RPA. Kaplan-Meier curves and risk table in the evaluation set of 350 patients with another glioma for risk groups 1-4 are defined by the training set in Figure 4, A. Astro = astrocytoma; GBM = glioblastoma; Oligo = oligodendroglioma.

blood-based immune markers as an additional tool for glioma survival risk prediction.

Funding

This work was supported by the National Institutes of Health (grant numbers R01CA52689, P50CA097257, R01CA126831, R01CA139020, R25CA112355, and R01CA207360), the loglio Collective, and the National Brain Tumor Foundation and by donations from families and friends of John Berardi, Helen Glaser, Elvera Olsen, Raymond E. Cooper, and William Martinusen. JKW is supported by the Robert Magnin Newman Endowed Chair in Neuro-oncology and MW by the Stanley D. Lewis and Virginia S. Lewis Endowment. DCK was supported by NIH grants P30 CA168524 and P20 GM130423, and P20GM103428. LAS is supported by NIGMS grant P20GM1044168299 and CDMRP/DoD grant W81XWH-20-1-0778. KTK was supported by a 2018 AACR-Johnson & Johnson Lung Cancer Innovation Science grant (18-90-52-MICH).

Notes

Role of the funder: The funder had no role in the design of the study, collection of data, analysis and interpretation of the data, the writing of the manuscript, or the decision to submit the manuscript for publication.

Disclosures: JKW and KTK are co-founders of Cellintec, which had no role in this research. JLC receives research funding from Agios and Merck and is a consultant for Agios (not directly related to this study). JWT receives research support from AbbVie, Agios, BMS, and Navio. MW is a member of the board of directors of the Central Brain Tumor Registry of the United States (unpaid position). BC is a paid consultant on R01CA207360 (Immune Epigenetic Biomarkers of Survival in Glioma Epidemiology). All other authors have no disclosures.

Author contributions: Conceptualization: AMM, JKW, DCK, LAS, BCC, MW, KK, JWT, JLC. Methodology: AMM, GW, JYL, DCK, PC, HH, LAS, BCC, MW, KTK. Writing—Original draft: AMM, JKW, GW. Writing—Reviewing and editing: AMM, JKW, GW, JYL, DCK, PC, HH, SL, JA, TR, PB, LM, LAS, BCC, MW, KTK, JWT, JLC.

All authors were involved in the writing of the manuscript and have read and approved the final version.

Acknowledgements: The authors wish to acknowledge study participants, the clinicians, and research staff at the participating medical centers; the UCSF Helen Diller Family Comprehensive Cancer Center Genome Analysis Core, which is supported by a National Cancer Institute Cancer Center Support Grant (5P30CA082103); the UCSF Cancer Registry (for updating UCSF glioma case survival and vital status); and the UCSF Neurosurgery Tissue Bank. We thank William Karlon, MD, PhD, for his flow cytometry expertise.

Disclaimers: This publication was supported by the National Center for Research Resources and the National Center for Advancing Translational Sciences, National Institutes of Health, through UCSF-CTSI Grant Number UL1 RR024131. Its contents are solely the responsibility of the authors and do not necessarily represent the official views of the National Institutes of Health. The collection of cancer incidence data used in this study was supported by the California Department of Public

Health pursuant to California Health and Safety Code Section 103885; Centers for Disease Control and Prevention's National Program of Cancer Registries, under cooperative agreement 5NU58DP006344; the National Cancer Institute's Surveillance, Epidemiology, and End Results Program under contract HHSN261201800032I awarded to UCSF, contract HHSN261201800015I awarded to the University of Southern California, and contract HHSN261201800009I awarded to the Public Health Institute, Cancer Registry of Greater California. The ideas and opinions expressed herein are those of the authors and do not necessarily reflect the opinions of the state of California, Department of Public Health, the National Cancer Institute, and the Centers for Disease Control and Prevention or their contractors and subcontractors. All analyses, interpretations, and conclusions reached in this manuscript from the mortality data are those of the authors and not the state of California Department of Public Health.

Prior presentations: This research was presented as an on-demand prerecorded oral presentation at the Society for Neuro-oncology Annual Meeting (November 19-22, 2020).

Data Availability

Methylation and phenotype data used in this manuscript will be available through dbGaP Study Accession phs001497.v2.p1. Participant-level information about subtype, gender, age, DNAmAge, HannumAge, and DNAmPhenoAge, with a sample ID link to the deposited dbGaP data, can be found in [Supplementary Table 10](#) (available online). Requests to access additional deidentified data used in this manuscript will be considered through a request to the corresponding author.

References

- Molinari AM, Taylor JW, Wiencke JK, Wrensch MR. Genetic and molecular epidemiology of adult diffuse glioma. *Nat Rev Neurol*. 2019;15(7):405–417.
- Eckel-Passow JE, Lachance DH, Molinari AM, et al. Glioma groups based on 1p/19q, IDH, and TERT promoter mutations in tumors. *N Engl J Med*. 2015;372(26):2499–2508.
- Louis DN, Perry A, Reifenberger G, et al. The 2016 World Health Organization classification of tumors of the central nervous system: a summary. *Acta Neuropathol*. 2016;131(6):803–820.
- Pekmezci M, Rice T, Molinari AM, et al. Adult infiltrating gliomas with WHO 2016 integrated diagnosis: additional prognostic roles of ATRX and TERT. *Acta Neuropathol*. 2017;133(6):1001–1016.
- The Cancer Genome Atlas Research Network; Brat DJ, Verhaak RG, Aldape KD, et al. Comprehensive, integrative genomic analysis of diffuse lower-grade gliomas. *New Engl J Med*. 2015;372(26):2481–2498. [10.1056/NEJMoa1402121] [26061751]
- Delgado-López PD, Corrales-García EM. Survival in glioblastoma: a review on the impact of treatment modalities. *Clin Transl Oncol*. 2016;18(11):1062–1071.
- Curran WJ Jr, Scott CB, Horton J, et al. Recursive partitioning analysis of prognostic factors in three Radiation Therapy Oncology Group malignant glioma trials. *J Natl Cancer Inst*. 1993;85(9):704–710.
- Scott CB, Scarantino C, Urtasun R, et al. Validation and predictive power of Radiation Therapy Oncology Group (RTOG) recursive partitioning analysis classes for malignant glioma patients: a report using RTOG 90-06. *Int J Radiat Oncol Biol Phys*. 1998;40(1):51–55.
- Paravati AJ, Heron DE, Landsittel D, et al. Radiotherapy and temozolomide for newly diagnosed glioblastoma and anaplastic astrocytoma: validation of Radiation Therapy Oncology Group-Recursive Partitioning Analysis in the IMRT and temozolomide era. *J Neurooncol*. 2011;104(1):339–349.
- Bell EH, Zhang P, Fisher BJ, et al. Association of MGMT promoter methylation status with survival outcomes in patients with high-risk glioma treated with radiotherapy and temozolomide: an analysis from the NRG oncology/RTOG 0424 trial. *JAMA Oncol*. 2018;4(10):1405–1409.
- Molinari AM, Hervey-Jumper S, Morshed RA, et al. Association of maximal extent of resection of contrast-enhanced and non-contrast-enhanced tumor with survival within molecular subgroups of patients with newly diagnosed glioblastoma. *JAMA Oncol*. 2020;6(4):495–503.

12. Ladomersky E, Scholtens DM, Kocherginsky M, et al. The coincidence between increasing age, immunosuppression, and the incidence of patients with glioblastoma. *Front Pharmacol.* 2019;10:200.
13. Pawelec G. Age and immunity: what is “immunosenescence”? *Exp Gerontol.* 2018;105:4–9.
14. Field AE, Robertson NA, Wang T, Havas A, Ideker T, Adams PD. DNA methylation clocks in aging: categories, causes, and consequences. *Mol Cell.* 2018; 71(6):882–895.
15. Goronzy JJ, Weyand CM. T cell development and receptor diversity during aging. *Curr Opin Immunol.* 2005;17(5):468–475.
16. Goronzy JJ, Fang F, Cavanagh MM, Qi Q, Weyand CM. Naive T cell maintenance and function in human aging. *J Immunol.* 2015;194(9):4073–4080.
17. Silva SL, Sousa AE. Establishment and maintenance of the human naïve CD4(+) T-cell compartment. *Front Pediatr.* 2016;4:119.
18. de Haan G, Lazare SS. Aging of hematopoietic stem cells. *Blood.* 2018;131(5): 479–487.
19. Geiger H, de Haan G, Florian MC. The ageing haematopoietic stem cell compartment. *Nat Rev Immunol.* 2013;13(5):376–389.
20. Aiello A, Farzaneh F, Candore G, et al. Immunosenescence and its hallmarks: how to oppose aging strategically? A review of potential options for therapeutic intervention. *Front Immunol.* 2019;10:2247.
21. Alpert A, Pickman Y, Leipold M, et al. A clinically meaningful metric of immune age derived from high-dimensional longitudinal monitoring. *Nat Med.* 2019;25(3):487–495.
22. Salas LA, Wiencke JK, Koestler DC, Zhang Z, Christensen BC, Kelsey KT. Tracing human stem cell lineage during development using DNA methylation. *Genome Res.* 2018;28(9):1285–1295.
23. Houseman EA, Accomando WP, Koestler DC, et al. DNA methylation arrays as surrogate measures of cell mixture distribution. *BMC Bioinformatics.* 2012;13:86.
24. Accomando WP, Wiencke JK, Houseman EA, Nelson HH, Kelsey KT. Quantitative reconstruction of leukocyte subsets using DNA methylation. *Genome Biol.* 2014;15(3):R50.
25. Hannum G, Guinney J, Zhao L, et al. Genome-wide methylation profiles reveal quantitative views of human aging rates. *Mol Cell.* 2013;49(2):359–367.
26. Horvath S. DNA methylation age of human tissues and cell types. *Genome Biol.* 2013;14(10):R115.
27. Levine ME, Lu AT, Quach A, et al. An epigenetic biomarker of aging for lifespan and healthspan. *Aging (Albany NY).* 2018;10(4):573–591.
28. Liao P, Ostrom QT, Stetson L, Barnholtz-Sloan JS. Models of epigenetic age capture patterns of DNA methylation in glioma associated with molecular subtype, survival, and recurrence. *Neuro Oncol.* 2018;20(7):942–953.
29. Wrensch M, Rice T, Miike R, et al. Diagnostic, treatment, and demographic factors influencing survival in a population-based study of adult glioma patients in the San Francisco Bay Area. *Neuro Oncol.* 2006;8(1):12–26.
30. Wiencke JK, Koestler DC, Salas LA, et al. Immunomethylomic approach to explore the blood neutrophil lymphocyte ratio (NLR) in glioma survival. *Clin Epigenetics.* 2017;9:10.
31. Koestler DC, Jones MJ, Usset J, et al. Improving cell mixture deconvolution by identifying optimal DNA methylation libraries (IDOL). *BMC Bioinformatics.* 2016;17(1):120.
32. Salas LA, Koestler DC, Butler RA, et al. An optimized library for reference-based deconvolution of whole-blood biospecimens assayed using the Illumina HumanMethylationEPIC BeadArray. *Genome Biol.* 2018;19(1):64.
33. Lostritto K, Strawderman RL, Molinaro AM. A partitioning deletion/substitution/addition algorithm for creating survival risk groups. *Biometrics.* 2012; 68(4):1146–1156.
34. Molinaro AM, Lostritto K, van der Laan M. partDSA: deletion/substitution/addition algorithm for partitioning the covariate space in prediction. *Bioinformatics.* 2010;26(10):1357–1363.
35. Uno H, Claggett B, Tian L, et al. Moving beyond the hazard ratio in quantifying the between-group difference in survival analysis. *J Clin Oncol.* 2014;32(22): 2380–2385.
36. R: A Language and Environment for Statistical Computing [computer program]. Vienna, Austria: R Foundation for Statistical Computing; 2020. <https://www.R-project.org/>.
37. Templeton AJ, McNamara MG, Seruga B, et al. Prognostic role of neutrophil-to-lymphocyte ratio in solid tumors: a systematic review and meta-analysis. *J Natl Cancer Inst.* 2014;106(6):dju124.
38. Capper D, Jones DTW, Sill M, et al. DNA methylation-based classification of central nervous system tumours. *Nature.* 2018;555(7697):469–474.
39. Grossman SA, Ye X, Lesser G, et al.; NABTT CNS Consortium. Immunosuppression in patients with high-grade gliomas treated with radiation and temozolomide. *Clin Cancer Res.* 2011;17(16):5473–5480.
40. Hughes MA, Parisi M, Grossman S, Kleinberg L. Primary brain tumors treated with steroids and radiotherapy: low CD4 counts and risk of infection. *Int J Radiat Oncol Biol Phys.* 2005;62(5):1423–1426.
41. Dix AR, Brooks WH, Roszman TL, Morford LA. Immune defects observed in patients with primary malignant brain tumors. *J Neuroimmunol.* 1999;100(1–2): 216–232.
42. Chongsathidkiet P, Jackson C, Koyama S, et al. Sequestration of T cells in bone marrow in the setting of glioblastoma and other intracranial tumors [published correction appears in *Nat Med.* 2019;25(3):529]. *Nat Med.* 2018;24(9): 1459–1468.
43. Mason M, Maurice C, McNamara MG, et al. Neutrophil-lymphocyte ratio dynamics during concurrent chemo-radiotherapy for glioblastoma is an independent predictor for overall survival. *J Neurooncol.* 2017;132(3): 463–471.
44. Lesterhuis WJ, Bosco A, Millward MJ, Small M, Nowak AK, Lake RA. Dynamic versus static biomarkers in cancer immune checkpoint blockade: unravelling complexity. *Nat Rev Drug Discov.* 2017;16(4):264–272.
45. Hartmann FJ, Bendall SC. Immune monitoring using mass cytometry and related high-dimensional imaging approaches. *Nat Rev Rheumatol.* 2020;16(2): 87–99.
46. Spitzer MH, Carmi Y, Reticker-Flynn NE, et al. Systemic immunity is required for effective cancer immunotherapy. *Cell.* 2017;168(3):487–502.e15.
47. Yost KE, Satpathy AT, Wells DK, et al. Clonal replacement of tumor-specific T cells following PD-1 blockade. *Nat Med.* 2019;25(8):1251–1259.
48. Krieg C, Nowicka M, Guglietta S, et al. High-dimensional single-cell analysis predicts response to anti-PD-1 immunotherapy [published correction appears in *Nat Med.* 2018;24(11):1773–1775]. *Nat Med.* 2018;24(2):144–153.
49. Iwahori K, Shintani Y, Funaki S, et al. Peripheral T cell cytotoxicity predicts T cell function in the tumor microenvironment. *Sci Rep.* 2019;9(1):2636.
50. Cloughesy TF, Mochizuki AY, Orpilla JR, et al. Neoadjuvant anti-PD-1 immunotherapy promotes a survival benefit with intratumoral and systemic immune responses in recurrent glioblastoma. *Nat Med.* 2019;25(3): 477–486.